Reluctance Network Analysis of an Orthogonal-Core Type Parametric Induction Motor

Katsubumi Tajima, Kohei Sato, and Toshihiko Komukai
Dept. of Electrical and Electronics Engineering, Akita University, 1-1 Tegata Gakuencho, Akita 010-8502, Japan

Osamu Ichinokura
Dept. of Electrical Engineering, Tohoku University, Aramaki Aza Aoba, Sendai 980-8579, Japan

Abstract—In this paper, an analytical method of an orthogonal-core type parametric induction motor is proposed, based on a reluctance network model of the stator. The model is derived by a similar technique applied to an orthogonal-core transformer. Using this model the parametric oscillation characteristic of the motor, without a rotor, is computed. The simulation results agree well with the experiments. It is obvious that the analytical model of the stator presented here is proper for analysis of the motor and that, by use of this model and suitable analytical model of the rotor, the motor characteristics can be analyzed.

Index Terms — Nonlinear magnetics, orthogonal-core, parametric motor, reluctance network analysis.

I. Introduction

Nonlinear magnetic devices, e.g. an orthogonal-core transformer [1]-[3] and parametric motor [4], have many applications because the devices have various attractive features. However, quantitative analysis of the devices is not easy because the flux distribution is generally intricate due to magnetic saturation. For optimum design of the devices, it is necessary to calculate the behavior characteristics from the properties of the core material and core dimensions.

Recently, the authors proposed an analytical method for the orthogonal-core transformer by use of a reluctance network [1]-[3]. This method is very accuracy, fast and easy. So, in this paper, this method is applied to the analysis of an orthogonal-core type parametric induction motor as a nonlinear magnetic device.

II. Basic Operation of Parametric Motor

Fig. 1 shows a schematic diagram of an orthogonal-core type parametric induction motor [4]. In the figure, the stator is constructed from two C-cores A_1, A_2 of identical shape and a toroidal core B. A_1 and A_2 are the primary and secondary magnetic circuits for excitation and are 90 degrees relative to each other in space. N_1 and N_2 are the primary and secondary windings. B is a common magnetic circuit for generating a rotating field. D is a rotor and C is a tuning capacitor.

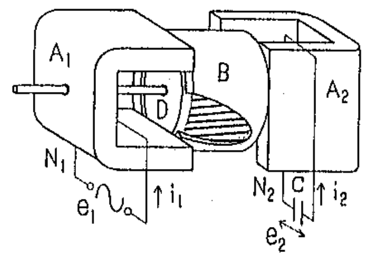

Fig. 1. Schematic diagram of the parametric induction motor.

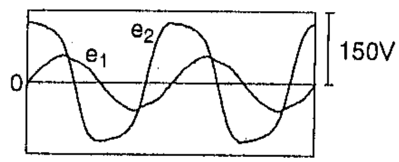

(C= 107.7μF, E_1 = 40 V, f = 50 Hz)

Fig. 2. Observed waveforms of generated voltage e_2.

When AC voltage e_1 is applied to the primary circuit, parametric oscillation is caused by magnetic saturation of the stator core and AC voltage e_2 is generated in the secondary circuit. Fig. 2 shows the observed waveforms of e_2. As the phase difference between e_2 and e_1 is almost 90 degrees, the motor acts as a 2-phase induction motor [4]. i_1 and i_2 are the primary and secondary currents.

Fig. 3 shows the dimensions of the stator core, and Fig. 4 illustrates the flux flows in the stator. In the Fig. 4, ϕ_1 and ϕ_2 are the primary and secondary fluxes, respectively. The flux distribution in the stator core is intricate due to its peculiar magnetic circuit and nonlinear magnetic property. Thus the quantitative analysis of the motor is not easy .

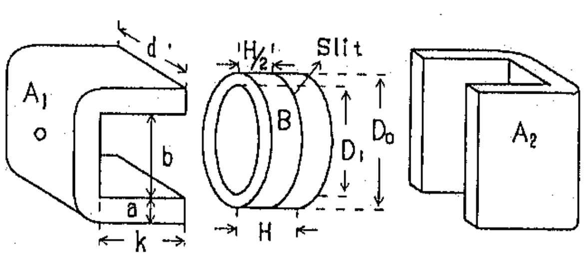

Fig. 3. Dimensions of the stator core.

Manuscript received March 5, 1999.

K. Tajima, +81 – 18 – 889 – 2333, fax +81 – 18 – 837 – 0406, tajima@ipc.akita-u.ac.jp; O. Ichinokura, +81 – 22 – 217 – 7053, fax +81 – 22 – 263 – 9286, ichinoku@ecei.tohoku.ac.jp.

0018-9464/99$10.00 © 1999 IEEE

Authorized licensed use limited to: TOHOKU UNIVERSITY. Downloaded on October 8, 2008 at 01:59 from IEEE Xplore. Restrictions apply.

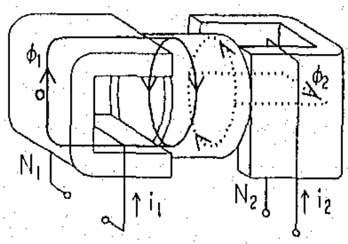

Fig. 4. Flux flow in the stator core.

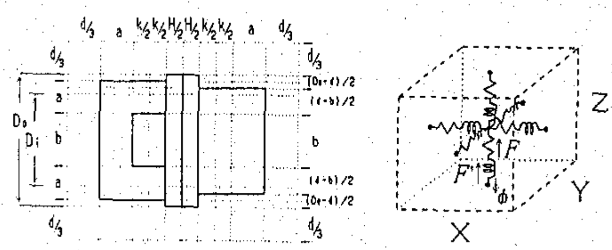

(a) Division. (b) Magnetic circuit for each element.

Fig. 5. Explanation for obtaining the reluctance network.

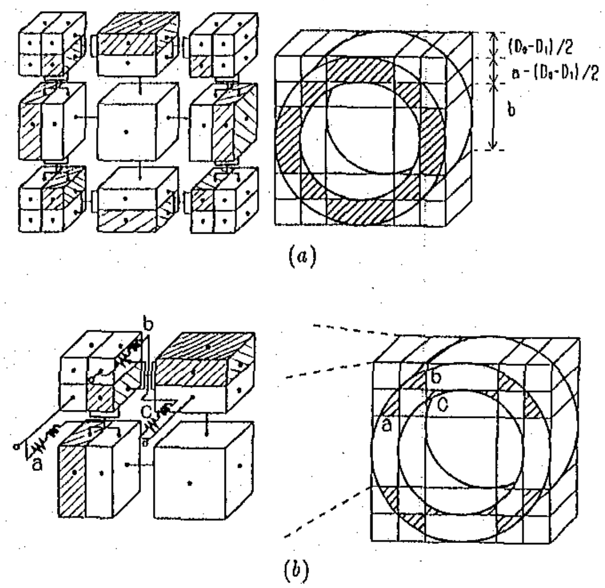

Fig. 6. Division of the toroidal core.

III. Analytical Method

In past work, the authors proposed an analytical method for an orthogonal-core transformer. This is a nonlinear magnetic device, based on a reluctance network model [1],[3]. In this paper, the reluctance network analysis is applied to the parametric motor. To evaluate the reluctance network model, the core has been divided into some rectangular prism elements [1],[3]. Fig. 5(a) and (b) show the division of the stator and the assumed magnetic circuit of each element. In Fig. 5(b), the reluctances and inductances express the magnetic saturation and hysteresis of the core. F is the MMF of the reluctance and F' is the MMF of the inductance. The character of the reluctances and inductances are determined by the dimensions X, Y and Z of the element, and nonlinear property of the material as follows:

$$F = \frac{Z}{2}\{\alpha_1 \frac{\phi}{XY} + \alpha_m (\frac{\phi}{XY})^m\} \qquad (1)$$

$$F' = \frac{Z}{2}\{\beta_1 \frac{1}{XY}\frac{d\phi}{dt} + \beta_n (\frac{1}{XY})^n (\frac{d\phi}{dt})^n\} \qquad (2)$$

where α_1, α_m, β_1, β_n are unique constants for core material and m, n are the odd numbers of m, n $\geq$ 3 [3]. By connecting the magnetic circuits of the elements adjoining each other, the reluctance network model can be obtained.

The toroidal core is expressed, approximately. The division rectangular prism elements into shadowed rectangular prism elements shown in Fig.6(a). As the circumferential flux flow of the toroidal core is considered, the magnetic circuits of some elements are connected in parallel. The axial sectional area of the shadowed elements are decided by the actual sectional area of the toroidal core. In addition, in Fig. 6(b) the magnetic circuits for the shadowed areas ignored in Fig. 6(a) are added to the reluctance network.

IV. Results and Discussion

Using the reluctance network model of the stator obtained, we compute the parametric oscillation characteristics of the motor without rotor.

Fig. 7 shows schematic of a circuit for analysis [2]. Fig. 7(a) shows the reluctance network model for the stator with MMFs due to the windings. The MMF is assumed to be concentrated, ignoring the spatial distribution. Using this reluctance network, the primary and secondary fluxes ϕ_1, ϕ_2 from the MMFs $N_1 i_1/2$, $N_2 i_2/2$ are calculated. Fig. 7(b) is the external electric circuits of the motor. R is the resistance to stabilize the parametric oscillation. r_1 and r_2 are the primary and secondary winding resistances.

By use of SPICE, one of the general circuit simulator, we can compute the circuit coupling the reluctance network of the stator with external electric circuits. The dimensions and materials of the stator core are shown in Table I. It is necessary to take account of the magnetic anisotropy including the laminated direction. Figs. 8 and 9 show the B-H curve and W_i-B_m characteristic of the core material. In the figure, catalog data [5] is used as measured data.

Fig. 10 shows the observed and calculated waveforms of e_2 and Fig. 11 shows the E_1-E_2 characteristics. As can be seen on the figures, good agreement is obtained between the simulation and experimental results.

V. Conclusion

The analytical model of the stator of the parametric motor proposed here appears to be proper. And by use

Authorized licensed use limited to: TOHOKU UNIVERSITY. Downloaded on October 8, 2008 at 01:59 from IEEE Xplore. Restrictions apply.

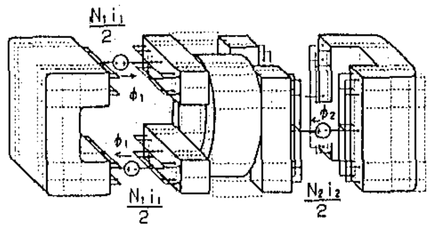

(*a*) Reluctance network model of the motor without rotor.

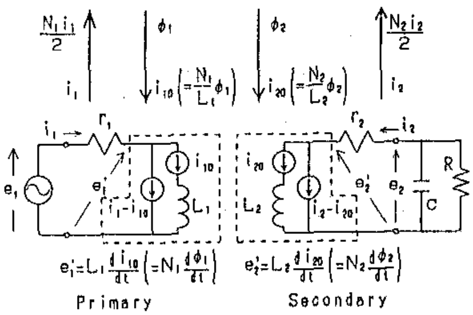

(*b*) External electrical circuit.

Fig. 7. Circuits for analysis.

TABLE I

Dimensions of the core and number of turns in the windings.

Core A1,A2	Dimensions [mm]	a=24.8, b=40.4, k=25.6, d=85.0
	Material	Grain oriented silicon steel strip with thickness of 0.18 mm
Core B	Dimensions [mm]	Do=100.4, Di=70.0, H=28.8
	Material	Grain oriented silicon steel strip with thickness of 0.18 mm
Winding [turns]		N1=200, N2=200
Winding resistances [Ω]		Primary : 0.676, Secondary : 0.676

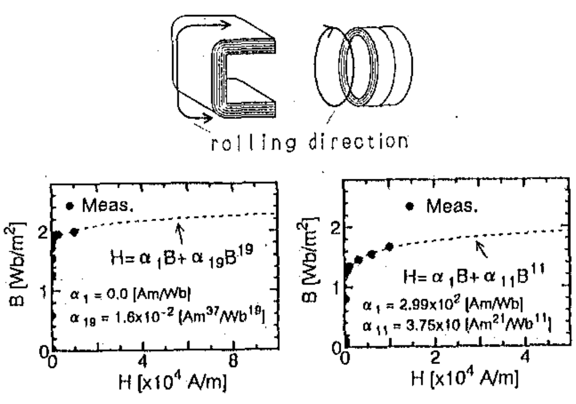

(*a*) Rolling direction. (*b*) Perpendicular direction.

Fig. 8. B-H curve of the core material.

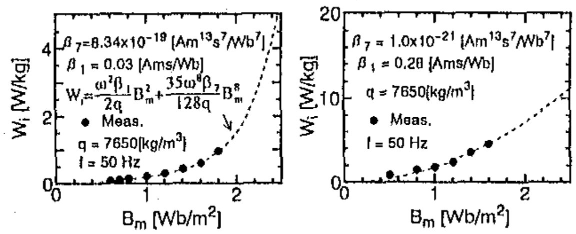

(*a*) Rolling direction. (*b*) Perpendicular direction.

Fig. 9. W_i-B_m characteristics of the core material.

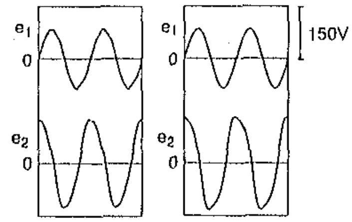

(a) Observed. (b) Simulation.

(C= 107.7μF, E_1 = 60 V, R = 400 Ω, f = 50 Hz)

Fig. 10. Observed and simulated waveforms of generated voltage e_2.

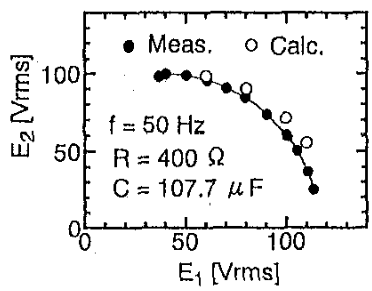

Fig. 11. E_1-E_2 characteristics.

of this model and suitable analytical model of the rotor, analysis of the motor characteristics is possible.

REFERENCES

[1] K. Tajima, O. Ichinokura, A. Kaga, and Y. Anazawa, "One method for calculating flux-MMF relationship of orthogonal-core," *IEEE Trans., Magn.*, vol. 29, pp. 3219–3221, 1993.

[2] K. Tajima, A. Kaga, and O. Ichinokura, "Performance analysis of the orthogonal-core type converters based on a circuit system combined with the reluctance network model of the orthogonal-core and the outer electric circuits," *T. IEE Japan*, vol. 117-A, pp. 155–160, 1997.

[3] K. Tajima, Y. Anazawa, T. Komukai, and O. Ichinokura, "An analytical method for characteristics of orthogonal-core under consideration of magnetic saturation and hysteresis," *7th EPE'97*, 2.006–2.011, 1997.

[4] Y. Sakamoto, M. Natsusaka, and K. Murakami, "A low noise slotless parametric motor suited for use in quiet environment," *IEEE Trans., Magn.*, vol. 28, pp.3000–3002, 1992.

[5] Nippon Steel, *Cat. No. SC503 63.3,*, 1992.

Authorized licensed use limited to: TOHOKU UNIVERSITY. Downloaded on October 8, 2008 at 01:59 from IEEE Xplore. Restrictions apply.